URANS Simulations for a Flooded Ship in Calm Water and Regular Beam Waves

Hamid Sadat-Hosseini, *IIHR – Hydroscience & Engineering*, hamid-sadathosseini@uiowa.edu
Dong-Hwan Kim, *IIHR – Hydroscience & Engineering*, donghwan-kim@uiowa.edu
Pablo Carrica, *IIHR – Hydroscience & Engineering*, pablo-carrica@uiowa.edu
Shin Hyung Rhee, *Seoul National University Towing Tank*, shr@snu.ac.kr
Frederick Stern, *IIHR – Hydroscience & Engineering*, frederick-stern@uiowa.edu

ABSTRACT

CFD simulations are conducted for zero-speed damaged passenger ship SSRC in calm water and waves with 6DOF motions including flooding procedure in calm water, roll decay in calm water and motions in regular beam waves for various wavelengths. The simulations model the 6DOF soft spring experimental mount, the one- and two-room flooding compartment configurations, including both intact and damaged conditions. For flooding and roll decay, simulations show ability predict the trend of increases in roll period and damping due to flooding, as reported in ITTC (2002). The damping magnitudes were often under-predicted with large errors while the roll period and compartment water height were well predicted. Two-room compartment simulation showed three times larger damping than one-room compartment cases whereas the roll period was similar for both conditions. For wave cases, all motions show primarily 1st order response, except for parametric roll condition which shows large ½ harmonic response for the intact ship. The 2nd order responses are small for both damaged and intact ship. The larger roll period and damping for the damaged ship shift the peak of responses to smaller wave frequency and reduce the amplitude of responses. The average error is often large for 1st order intact ship pitch and damaged ship surge and pitch and for most ½ and 2nd order responses. Large errors could be partially due to the complex mounting system in the experiment. Overall, current CFD results show better predictions than those reported for potential flow solvers even though the computational cost is larger.

Keywords: *CFD, Damage Ship Stability, Calm Water, Beam Waves*

1. INTRODUCTION

Safety is of high priority in ship design but poorly understood and often in conflict other important requirements such as powering, seakeeping and maneuvering. To meet new energy efficiency IMO guidelines requires a reduction in the main engine output. However, lowering output may result in diminished seakeeping and maneuvering performance. Finalization of the guidelines for minimum power requirement is in progress. Intact/damaged and static/dynamic stability are all major concerns.

Damaged dynamic stability is most complex and been research focus as summarized by the last several ITTC Stability in Waves Committee and Specialist Committee Reports. Flooding process, floodwater dynamics and ship motions are studied. Passenger and ferry ships are specified as benchmarks for experimental and simulation studies. For the zero-speed calm water damaged condition, the roll period and damping are larger than for the damaged condition. Increasing KG showed larger roll period and smaller damping and increasing floodwater height showed both larger roll period and damping. Tests for regular and

irregular waves indicated second harmonic roll motion and capsize, respectively. Recent focus is on time to flood and safe return to port and survival boundaries in irregular waves.

Potential flow methods are the common numerical approach to study the damaged ship stability (Papanikolaou et al., 2000; Palazzi and De Kat, 2004). The 6DOF damaged ship motions in waves are solved by various strip theory or panel based methods. The viscous effects are treated by semi-empirical approaches. The inflow and outflow of water through the openings is computed by the Bernoulli based equations including orifice, sluice gate and weir equations. The non-linear sloshing effect inside the compartment is often neglected, and the internal water surface is assumed to be either horizontal or a freely movable plane. The capability of potential flow methods for a damaged passenger ship (PRR1) with zero-speed was evaluated in 23rd ITTC Specialist Committee on Prediction Methods of Extreme Ship Motions and Capsize using several benchmark experimental data for free roll decay in calm water, motion in regular waves and survivability boundaries in irregular waves (ITTC, 2002). The potential flow predictions were only assessed for motions and not evaluated for floodwater height. The results from several potential flow tools showed overestimation of the damped roll frequency (E=-22%D) and underestimation of logarithmic roll damping coefficient (E=62%D) for roll decay, scattered results for regular waves with large over prediction for roll frequency (E=-15%D) and amplitude (E=-91%D), and only qualitative agreement with experimental data in irregular waves. Note that the comparison errors were not given in ITTC report and calculated by authors as E=(D-S)%D between the experimental data (D) and simulation (S) values.

The CFD study of the damaged ship is performed for very limited cases. Few studies only used CFD to predict the dynamic effect of floodwater and then coupled with the potential flow solvers for ship motion prediction (Strasser et al., 2009; Gao et al., 2013). Therefore, the accuracy of the predicted motions was still associated with the level of nonlinearity implemented in the potential flow solver. The complete physics-based CFD simulations are conducted only for the ship in calm water with semi-captive condition. Gao and Vassalos (2011) demonstrated the capability of CFD prediction for roll decay prediction of a damaged ship for initial angle ±5°. The simulations were conducted for 1DOF and 2DOF conditions with free roll motion w/ or w/o sway motion. Gao et al. (2011) validated motions and floodwater heights for 3DOF damaged barge in calm water free to heave, roll and pitch. The time history of roll motion showed quite large error (E~200%D) during the initial part of the flooding procedure while it is predicted well after the compartment is fully flooded. Additionally, the heave and pitch motions were well predicted with E<5%D. The trends of computed floodwater heights were generally consistent with the experimental measurements. However, there were differences between numerical simulation and experiment which could not be quantified.

Herein, the capabilities of physics-based CFD simulations are assessed for zero-speed ship flooding and roll decay in calm water and regular beam waves with 6DOF motions using the experimental data provided by Lee et al. (2015). The simulations model the soft spring experimental mount, the one- and two–room flooding compartment configurations, including both intact and damaged conditions. The errors are evaluated for floodwater and motions using the experimental data. The level of the errors is compared with that from previous potential flow studies and the cost and benefit for the current approach is described.

2. EXPERIMENTAL VALIDATION DATA

2.1 Facility, model, mount, measurement systems

The tests are conducted in the Seoul National University (SNU) towing tank, which

is 110 m long, 8 m wide and 3.5 m deep. A 1:82.75 scale, L=3.0 m geosim of the SSRC passenger ship is used for the experiments. Model-scale geometric parameters are summarized in Table 1. The model is appended with a compartment installed at the mid-ship as shown in Fig. 1a. The compartment is divided by a side wall into two rooms connected through a small hole, so that there is a cross-flooding between the rooms. Both compartment rooms have ventilation holes on their roof to have atmosphere pressure inside the rooms during flooding. The flooding occurs through a gate located on the starboard side of the compartment. The compartment layout is shown in Fig. 1b.

Table 1 The main particulars of SSRC

Description	Particulars
Ship Model	
Length between perpendiculars [m]	3
Beam (B/L) [-]	0.143
Draft (T/L) [-]	0.034
Damage length [m]	0.150
LCG/L [-]	0.520
KG/L [-]	0.032
Radius of gyration along x-axis [-]	0.053 (0.0501*)
Radius of gyration along y-axis [-]	0.250
Radius of gyration along z-axis [-]	0.250
Heave and pitch frequency	1.003 Hz
Roll frequency	0.487 Hz
Damaged Compartment	
Number of Rooms	Two
Compartment shape	Box
Ventilation hole	Yes
Opening door shape	Rectangular
Opening door length	0.0727
Opening door height	0.061

*adjusted k_{xx}

In the experiments, the ship was located in the mid-tank, free to all degree of motions. For wave cases, the aft and fore of the model were attached to the stationary carriage using four springs to compensate the drift motion of the ship in the experiment. All springs were initially installed to be parallel and close to the free surface. A simple mass-spring measurement showed that the spring force has linear behavior within the range of possible spring length during the experiment. The effective spring stiffness is shown to be 5.946 N/m and the spring forces are off by 6.8148 N from the one estimated by F=kx. For flooding of the compartment, its gate was opened using an air cylinder that pulled up the gate in the vertical direction. The opening time was approximately 0.09 second in model scale and it was confirmed that the induced roll motion due to the opening mechanism was negligible.

Table 2 The EFD and CFD test matrix for SSRC

Type	ϕ_i (deg)	# of comp. room	sea condition	validation variables
Flooding	0.0	-	Calm water	ϕ, $\zeta_{A,B,C}$
Intact roll decay	-13.7 -20.5	-	Calm water	ϕ
Damaged roll decay	-15.6	1	Calm water	ϕ
	15.9	1		ϕ
	-25.5	1		ϕ, $\zeta_{A,B,C}$
	26.7	1		ϕ
	-28.6	2		ϕ, $\zeta_{A,B,C,D,E}$
Intact beam waves*	-	2	λ/L=0.52,1.17,1.99, 2.20,2.42 H/λ=1/60,1/100	x,y,z,ϕ,θ,ψ $\zeta_{A,B,C,D,E}$
Damaged beam waves*	-	2	λ/L=0.52,1.17,1.99 ,2.20,2.42 H/λ=1/60,1/100	x,y,z,ϕ,θ,ψ $\zeta_{A,B,C,D,E}$

*CFD simulations in waves are only conducted for H/l=1/60.

Two measurement systems were used for the experiments: flooding water and ship motion measurement systems. The height of the flooding water was measured by five capacitance type wave probes at locations A, B, C, D, E in the compartment (ζi; i=A,B,C,D,E) as shown in Fig. 1b. The 6DOF motion responses (x,y,z,ϕ,θ,ψ) were measured with a combination of the accelerometers and inertial measurement unit (IMU). The IMU was mainly used for the roll motion measurement in the free roll decay test. The accelerometers were used to obtain 6DOF motion responses from the test results in regular waves. From the measured accelerations, the 6DOF motion responses of the model were obtained using the strap-down method. It should be noted that the accelerations were first filtered using band-pass filtering in Matlab and then numerically

integrated to get velocities. The velocity data were filtered again and numerically integrated to produce displacement. Thus the experimental data reduction technique might have influence on the accuracy of the data. More details of the experimental setup and measurement system are reported in Lee et al. (2012, 2014) and Lim et al. (2015).

2.2 Conditions and validation variables

The experimental test matrices are provided in Table 2. The tests include flooding procedure in calm water for damaged SSRC, roll decay in calm water for intact and damaged SSRC, and motions in regular waves for intact and damaged SSRC. All tests were performed for zero Fr with free motions. Roll decay test were conducted by imposing different initial roll angle including ϕ_i=-13.7° and -20.5° for intact ship and about ϕ_i=±16° and ±26° (+15.9° and -15.6°; +26.7° and -25.5°) for the damaged ship with one-room compartment and ϕ_i=-28.6° with two-room compartment. The negative initial roll angle represents rolling toward the damaged side. The regular waves tests were conducted for two wave steepness conditions H/λ=1/100 and 1/60 as shown in Table 2. The wave periods were 1, 1.5, 1.995, 2.055, 2.155 sec, chosen to be distributed around the natural roll period of the intact SSRC which is 2.055 second (see Table 1). The wave periods correspond to λ/L=0.52, 1.17, 1.99, 2.2, 2.42. The wave heading was 270 deg (beam waves), approaching the ship from the damaged side. Both rooms were included in the damaged ship tests in waves.

As shown in Tables 2, the validation variables for calm water cases include ϕ and $\zeta_{A,B,C}$ for flooding and ϕ for all roll decay cases plus $\zeta_{A,B,C}$ and $\zeta_{A,B,C,D,E}$ for ϕ_i=-25.5° and -28.6°, respectively. For waves, the validation variables include x,y,z,ϕ,θ,ψ and $\zeta_{A,B,C,D,E}$.

3. COMPUTATIONAL METHODS

The code CFDShip-Iowa v4.5 (Huang et al., 2008) is used for the CFD computations. The simulations are conducted in absolute inertial earth-fixed coordinates. k-ε/k-ω with no wall function is used for turbulence model. A single-phase level-set method is used for free-surface capturing. The 6DOF rigid body equations of motion are solved to predict the ship motions. Dynamic overset grid technique is used to allow motions for the ship. The governing equations are discretized using finite difference schemes on body-fitted curvilinear grids. The time derivatives in the turbulence and momentum equations are discretized using second order finite Euler backward difference. Convection terms in the turbulence and momentum equations are discretized with higher order upwind formula. The viscous term in momentum and turbulent equations are computed with similar considerations using a second order difference scheme. Projection method, a two-stage fractional step scheme, is employed to couple pressure field and velocity effectively. In order to solve the system of discretized governing equations, between three and five inner iterations are used in each time step and solutions are considered to be converged once the error for velocities, pressure, and level set reach to less than 10-5, 10-8, and 10-5 respectively.

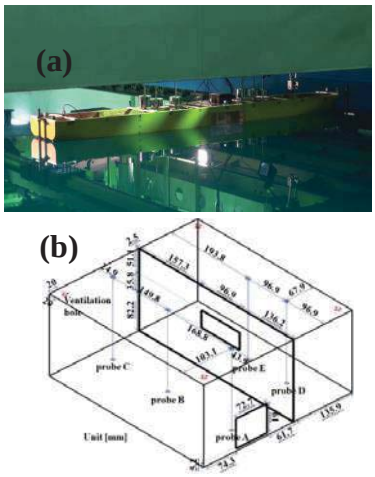

Figure 1 The damaged SSRC model: (a) SSRC hull geometry; (b) compartment layout.

3.1 Soft spring mount modeling

Similar to the experimental setup, springs were included in the regular wave simulations to counteract the wave drift forces while the

ship model is still free to all modes of motion. The spring forces for all 6DOF were computed in earth coordinate system and then transformed to ship-fixed coordinate system with origin at the center of gravity (G) to be considered in the equations of motion. The spring moments in ship-fixed coordinate were calculated by cross product of the moments' arm and forces described in ship-fixed coordinate.

The displacement of each spring was found in earth coordinate system based on the position of the two ends of that spring. For spring i, one end is attached to the ship at point P_i and another is attached to the carriage at point C_i. The location of P_i changes during simulation as it is located on the ship. The location of P_i in earth coordinate system was found based on:

$$\mathrm{r}_{Pi} = \mathrm{r}_G + \mathrm{R} \cdot \mathrm{d}_{Pi} \tag{1}$$

Here, r_{Pi} and d_{Pi} are the displacement vector of P_i in earth and ship coordinate system, r_G is the displacement vector of G in earth coordinate system, and R is the rotational matrix from ship to earth coordinate system.

The force for the i^{th} spring attached to the ship at point P_i and the carriage at C_i was calculated as follows:

$$\mathrm{F}_i = \frac{r_{Ci} - r_{Pi}}{\left| r_{Ci} - r_{Pi} \right|} \cdot f\left(r_{Ci} - r_{Pi} \right) \tag{2}$$

where, F_i is the force vector in earth coordinate system and f is the spring force function which is dependent on the spring displacement. In this study, the formula found from experiment is used.

The total spring induced forces in earth coordinate system (F) are sum of the forces induced by each spring as shown in Eq. (3). Then the total forces were transformed into ship coordinate system (Eq. (4)).

$$\mathrm{F} = \sum_{i=1}^{4} \mathrm{F}_i \tag{3}$$

$$\mathrm{F}' = \mathrm{R}^{-1} \cdot \mathrm{F} \tag{4}$$

where F' is the total spring induced forces in ship coordinate system.

For the spring moments, each spring force was transformed to ship coordinate system first and then the moment induced by each spring was calculated by cross product of the moments' arm and forces:

$$\mathrm{F}_i' = \mathrm{R}^{-1} \cdot \mathrm{F}_i \tag{5}$$

$$\mathrm{M}_i' = \left(\mathrm{r}_{Ci} - \mathrm{r}_{Pi} \right) \times F_i' \tag{6}$$

$$\mathrm{M}' = \sum_{i=1}^{4} \mathrm{M}_i' \tag{7}$$

After calculating the spring forces and moments in ship-fixed coordinates, they were added to the total forces and moments applied on the right hand side of the equations of motion. The total forces and moments are the fluid forces and moments integrated at each time step not only on the ship hull but also inside the flooded compartment. This means that the change of the ship mass and/or center of gravity due to the flooding are already included in the integrated forces and moments. Therefore, there's no need to modify the ship mass, moment of inertia or center of the gravity unlike the traditional methods. In the traditional methods, the flooded compartments are treated often as an additional weight to the ship. The added weight then changes the center of gravity and moments of inertia of the ship and consequently the equations of motion have to be solved for the ship with the new properties.

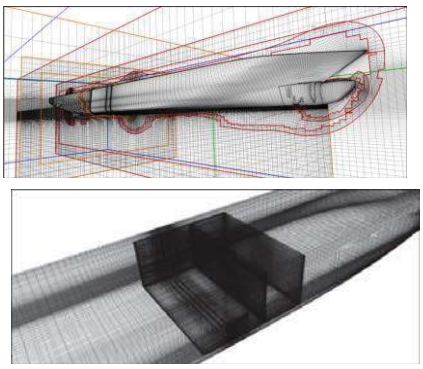

Figure 2 Grid topology for damaged SSRC and compartment.

3.2 Domain, boundary conditions, grids, conditions, and analysis method

The computational domain extends from -1.5<x<1.5, -1.2<y<1.2, -1<z<0.25 for roll decay and flooding procedure simulation and -1.5<x<1.5, -2<y<1, -1<z<0.25 for regular wave simulations of intact/damaged SSRC in dimensionless coordinates based on ship length. The ship axis is aligned with x with the bow at x=0 and the stern at x=1. The y axis is positive to starboard with z pointing upward. The free surface at rest lies at z=0.

Several types of boundary condition are used in this CFD study. The far field boundary conditions are imposed on the top and bottom of background. The no-slip condition is applied on the solid surfaces on the hull or inside the compartment. On the sides, the zero gradient boundary condition is applied. For calm water simulation, the inlet and exit boundary conditions are used for inlet and outlet of the domain. For waves, the inlet and outlet boundary conditions are calculated from the linear potential flow solution of waves.

Table 3 CFD and EFD comparison of roll motion for calm water cases

Type	ϕ_i	EFD/CFD	f_d			δ			α			$\bar{\phi}$	ϕ_m			Ave.
			f_d^p	f_d^s	Ave.	δ^p	δ^s	Ave.	α^p	α^s	Ave.		ϕ_m^p	ϕ_m^s	Ave.	
Flooding		EFD	0.452	0.439	0.446	0.083	0.201	0.142	0.037	0.088	0.063	-2.489	0.93	0.81	0.87	
		CFD	0.436	0.433	0.435	0.042	0.122	0.082	0.018	0.053	0.036	-2.472	2.68	2.58	2.63	
		E%D	**3.54**	**1.37**	**2.47**	**49.40**	**39.30**	**42.25**	**51.35**	**39.77**	**43.20**	**0.68**	**-188.17**	**-218.52**	**-202.30**	**65.78**
Intact Roll Decay	-13.7	EFD	0.489	0.488	0.489	0.181	0.193	0.187	0.089	0.094	0.092	0	8.24	9.25	8.75	
		CFD	0.486	0.487	0.487	0.120	0.096	0.108	0.058	0.057	0.058	0	9.14	9.1	9.12	
		E%D	**0.61**	**0.20**	**0.41**	**33.70**	**50.26**	**42.25**	**34.83**	**39.36**	**37.16**	**0.00**	**-10.92**	**1.62**	**-4.29**	**19.04**
	-20.5	EFD	0.493	0.492	0.493	0.267	0.241	0.254	0.132	0.119	0.126	0	12.48	11.81	12.15	
		CFD	0.490	0.488	0.489	0.242	0.187	0.215	0.119	0.091	0.105	0	13.18	11.73	12.46	
		E%D	**0.61**	**0.81**	**0.71**	**9.36**	**22.41**	**15.55**	**9.85**	**23.53**	**16.33**	**0.00**	**-5.61**	**0.68**	**-2.55**	**8.16**
	Ave. E%D		**0.61**	**0.51**	**0.56**	**21.53**	**36.33**	**28.90**	**22.34**	**31.45**	**26.75**	**0.00**	**8.27**	**1.15**	**110.19**	**13.60**
Damaged Roll Decay	-15.7	EFD	0.438	0.441	0.440	0.391	0.159	0.275	0.171	0.070	0.121	-2.897	5.74	10.39	8.07	
		CFD	0.444	0.442	0.443	0.255	0.128	0.192	0.114	0.057	0.086	-2.480	7.17	11.01	9.09	
		E%D	**-1.37**	**-0.23**	**-0.80**	**34.78**	**19.50**	**30.36**	**33.33**	**18.57**	**29.05**	**14.39**	**-24.91**	**-5.97**	**-12.71**	**17.13**
	15.9	EFD	0.438	0.437	0.438	0.336	0.193	0.265	0.147	0.084	0.116	-2.628	7.68	14.29	10.99	
		CFD	0.445	0.445	0.445	0.241	0.170	0.206	0.107	0.076	0.092	-2.354	8.08	13.93	11.01	
		E%D	**-1.60**	**-1.83**	**-1.71**	**28.27**	**11.92**	**22.31**	**27.21**	**9.52**	**20.78**	**10.43**	**-5.21**	**2.52**	**-0.18**	**11.04**
	-25.5	EFD	0.444	0.440	0.442	0.385	0.188	0.287	0.171	0.083	0.127	-2.932	11.07	14.61	12.84	
		CFD	0.432	0.444	0.438	0.363	0.233	0.298	0.157	0.103	0.130	-2.351	11.07	16.61	13.84	
		E%D	**2.70**	**-0.91**	**0.90**	**5.71**	**-23.94**	**-4.01**	**8.19**	**-24.10**	**-2.36**	**19.82**	**0.00**	**-13.69**	**-7.79**	**11.07**
	26.7	EFD	0.443	0.444	0.444	0.356	0.268	0.312	0.157	0.119	0.138	-2.474	9.87	17.24	13.56	
		CFD	0.445	0.431	0.438	0.285	0.164	0.225	0.127	0.071	0.099	-2.373	9.96	13.61	11.79	
		E%D	**-0.45**	**2.93**	**1.24**	**19.94**	**38.81**	**28.04**	**19.11**	**40.34**	**28.26**	**4.08**	**-0.91**	**21.06**	**13.06**	**16.46**
	-28.6	EFD	0.434	0.432	0.433	0.542	0.183	0.363	0.235	0.079	0.157	-5.843	8.04	17.37	12.71	
		CFD	0.402	0.416	0.409	0.439	0.184	0.312	0.176	0.077	0.127	-4.995	9.66	16.95	13.31	
		E%D	**7.37**	**3.70**	**5.54**	**19.00**	**-0.55**	**14.07**	**25.11**	**2.53**	**19.43**	**14.51**	**-20.15**	**2.42**	**-4.72**	**10.67**
	Ave. E%D		**2.70**	**1.92**	**2.04**	**21.54**	**18.94**	**19.76**	**22.59**	**19.01**	**19.97**	**12.65**	**10.24**	**9.13**	**7.69**	**13.28**

Table 4 CFD and EFD comparison of water height inside the compartment for calm water cases

Type	ϕ_i	EFD/CFD	ζ_A		ζ_B		ζ_C		ζ_D		ζ_E		Ave. $\bar{\zeta}$	Ave. f_ζ	Ave.
			$\bar{\zeta}_A$	f_{ζ_A}	$\bar{\zeta}_B$	f_{ζ_B}	$\bar{\zeta}_C$	f_{ζ_C}	$\bar{\zeta}_D$	f_{ζ_D}	$\bar{\zeta}_E$	f_{ζ_E}			
Flooding	0	EFD	0.080	0.465	0.071	0.441	0.064	0.465	no comp. #2		no comp. #2				
		CFD	0.078	0.444	0.071	0.435	0.064	0.424							
		E%D	**2.55**	**4.47**	**0.81**	**1.33**	**-0.39**	**8.74**					**1.25**	**4.85**	**3.05**
Damaged Roll Decay	-25.5	EFD	0.073	0.428	0.064	N/A	0.055	0.437	no comp. #2		no comp. #2				
		CFD	0.074	0.415	0.068		0.063	0.430							
		E%D	**-1.89**	**2.96**	**-6.49**		**-13.44**	**1.62**					**7.27**	**1.53**	**4.40**
	-28.6	EFD	0.089	0.446	0.062	N/A	0.059	0.426	0.089	0.440	0.077	N/A			
		CFD	0.086	0.402	0.072		0.061	0.419	0.083	0.413	0.075				
		E%D	**3.67**	**9.99**	**-16.27**		**-4.47**	**1.44**	**6.62**	**6.14**	**2.46**		**6.70**	**3.51**	**5.11**

The computational grids are overset, with independent grids assembled together to generate the total grid. The grid includes the ship hull boundary layer, compartment room 1 and 2, ventilation hole, connection grids, refinements, and background. The boundary layer grids are small enough (y+<1) to capture the boundary layer. Because the ship hull is symmetric respect to center-plane, the grid for one side of the ship was generated and then mirrored respect to center-plane. Two Cartesian grids are used for the inside of the rooms 1 and 2 of the compartment. Two connection grids are also used; one at the opening door located between the two rooms and another one located at the compartment door. A circular cylinder grid was designed for ventilation hole. Cartesian grids are used for several refinements around the ship. In addition, a Cartesian grid for background is used to impose the far-field boundary conditions. The grid size ranges from 2.4M to 28.5M depending on the damage/intact and calm water/wave conditions of the simulations. For calm water cases, the grid size is 6.3M for the intact ship and 19.8M and 28.5M for the damaged ship with one- and two-room compartment, respectively. For wave cases, the grid size for the intact ship is 7.09M-12.2M, finer for short wave cases. The grid size for the damaged ship is within 24.1M-27.1M grid points. For verification study, a fine grid with 19.9M and a coarse grid with 2.4M points are generated from the medium grid with 7.09M points using refinement/coarsen ratio of $\sqrt{2}$. The details of grid system for damaged SSRC with the two-room compartment are shown in Fig. 2.

For the coarse grid (2.4M), 32 CPUs have been employed in parallel running for 72 hours wall cock time with computational cost of 2300 CPUh. The computational cost increases with the increase of the grid size reaching to 97000 CPUh for the finest grid (28.5 M) as it requires 288 CPUs running for about 14 days. Compared to the presumably negligible computational cost for potential flow solvers, the computational cost for current CFD study is large but it is a complete physics-based method which can be used for much more complex conditions compared to potential flow.

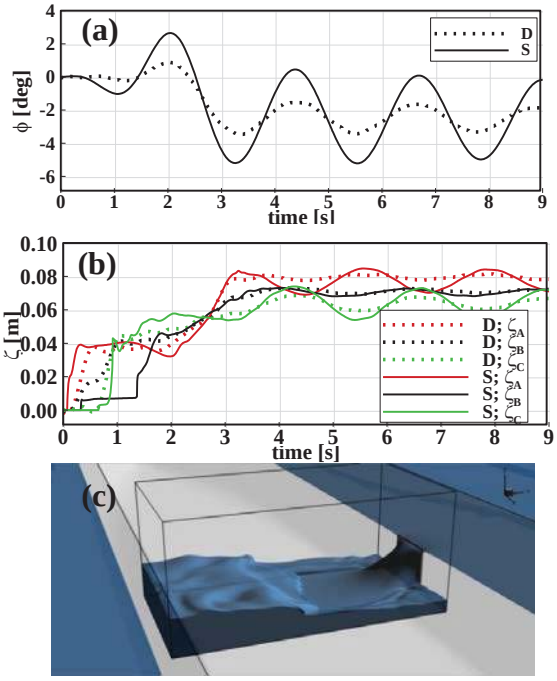

Figure 3 Flooding procedure for damaged SSRC in calm water: (a) roll; (b) floodwater height; (c) a snap shot of the predicted compartment flooding

The simulations are carried out in calm water and in waves, as shown in Table 2. The simulations are performed for the ship at zero Fr and free to all motions. For calm water, the flooding and intact/damaged roll decay cases with all different initial roll angles are simulated. For beam waves, the intact/damaged ship simulations are conducted only for the largest wave slope ($H/\lambda=1/60$) for $\lambda/L=0.52$, 1.17, 1.99, 2.2, 2.42. For all CFD simulations, k_{xx} value is adjusted to 0.0501L (see Table 1), found from preliminary roll decay simulation compared with the experimental data. It should be noted that experimental setup usually has difficulties to fix k_{xx} of the model to the desired value.

The validation variables are motions and water height as listed in Table 2. For flooding and roll decay, validation study is also conducted for the roll decay variables including mean roll angle (ϕ_{mk}), damping frequency (f_{dk}), logarithmic decrement (δ_k) and linear damping coefficient (α_k), and their averages over k roll

cycles (ϕ_m, f_d, δ, α), following roll decay analysis method described in Irvine et al. (2013). Harmonic analysis are conducted for the cases in beam waves.

4. VERIFICATION STUDY

Iterative U_I and grid U_G and time U_T size uncertainties were evaluated following Stern et al. (2001) and Xing and Stern (2010) for the intact configuration regular beam waves λ=2.4L and H/λ=1/60 conditions. The verification variables included the 1st harmonic amplitude of 6DOF motions (x_1,y_1,z_1,ϕ_1,θ_1,ψ_1) and corresponding phases ($x_{\varepsilon 1}$,$y_{\varepsilon 1}$,$z_{\varepsilon 1}$,$\phi_{\varepsilon 1}$,$\theta_{\varepsilon 1}$,$\psi_{\varepsilon 1}$).

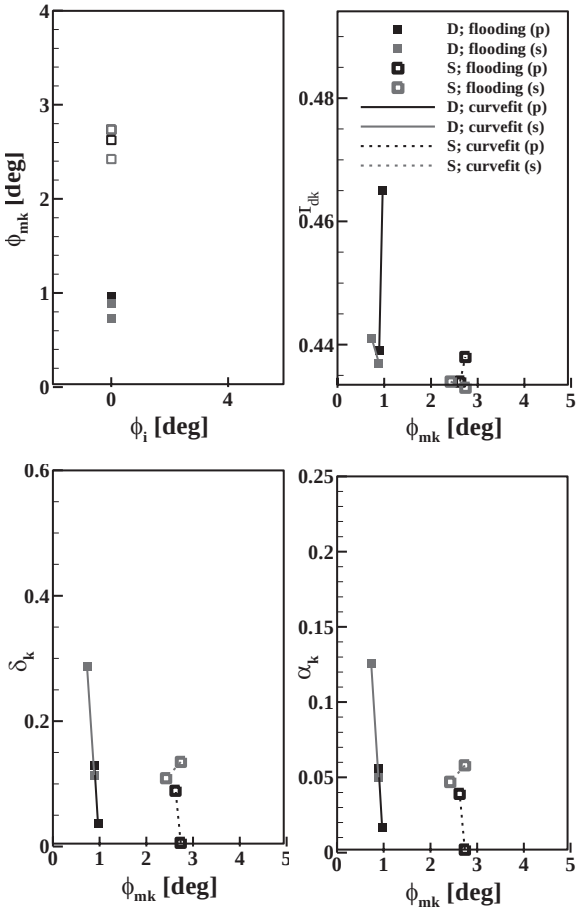

Figure 4 Variation of ϕ_{mk} with respect to ϕ_i and f_{dk},δ_k,α_κ with respect to ϕ_{mk} for flooding

The verification study showed U_I<2%S_1 for both 1st harmonic amplitudes and phases with average values 0.75 and 1.22, respectively. The largest U_I was for surge and heave motions i.e. x_1, z_1 and $x_{\varepsilon 1}$, $z_{\varepsilon 1}$. U_G/U_T were mostly MC and OC with small/large P values thus far from asymptotic range with average values 1.28/0.18 and 9.64/3.49 for amplitudes and phases, respectively. Similar to U_I, the largest U_G/U_T were for surge and heave motions. Average U_{SN} is 1.05 and 8.30 for amplitudes and phases, respectively. Further studies are needed for improved convergence and flooded conditions.

5. FLOODING

Fig. 3 shows a comparison of the experimental and computational roll and flooded compartment wave elevations along with a snap shot of the predicted compartment flooding.

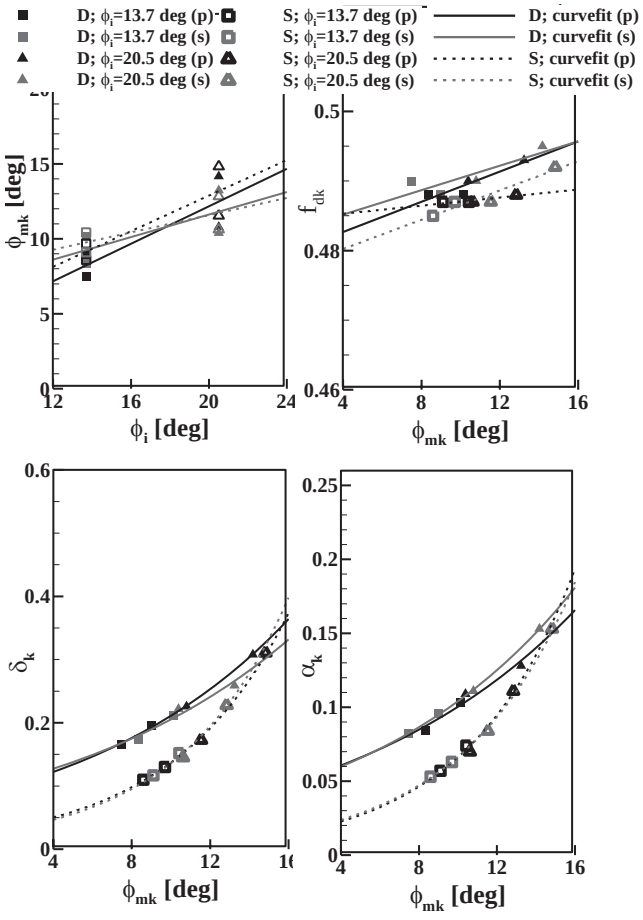

Figure 5 Variation of ϕ_{mk} with respect to ϕ_i and f_{dk},δ_k,α_κ with respect to ϕ_{mk} for intact roll decay

Fig. 4 shows comparison of the experimental and computational ϕ_{mk} vs. initial roll angle (ϕ_i) and f_{dk}, δ_k and α_k vs. ϕ_{mk}.

Values are shown for both the port and starboard sides since the damaged roll response is asymmetric.

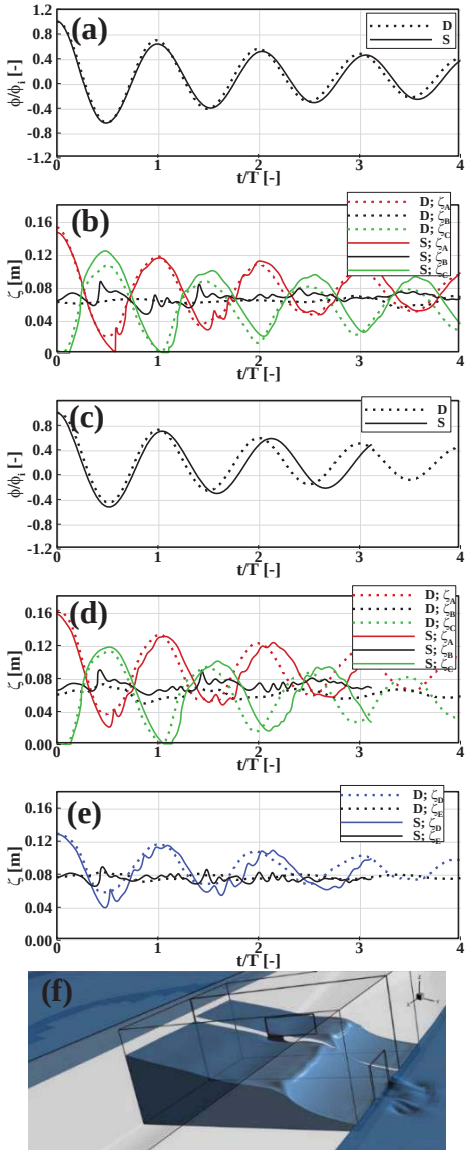

Figure 6 Results for damaged roll decay: (a) roll for ϕ_i=-25.5°; (b) floodwater height for ϕ_i=-25.5°; (c) roll for ϕ_i=-28.6°; (d) floodwater height in room #1for ϕ_i=-28.6°; (e) floodwater height in room #2 for ϕ_i=-28.6°; (f) a snap shot of the predicted two-room compartment flooding

Table 3 and 4 summarizes the values and comparison error for the validation variables which are averaged over roll cycles. For f_d, CFD shows similar values for the intact and damaged side (~0.43) while EFD shows slightly larger value for the intact side. The error for f_d is 3.5%D for the intact side and 1.37%D for the damaged side, showing that CFD can predict the damaged ship roll frequency quite well unlike the potential flow tools (ITTC, 2002). CFD results also show good agreement for heel angle E<1%D, and compartment wave elevation frequency/mean E<9%/3%D, but the linear damping are under predicted by E=43%D and consequently mean roll angle are predicted three times larger than EFD. The damped roll frequency is about 10% less than the one available for the intact ship roll decay, due to the lower GM value. Fig. 3c snap shot of the flooding compartment shows water entry with sloshing. The sloshing frequency is close to the damped roll frequency as shown in Table 4.

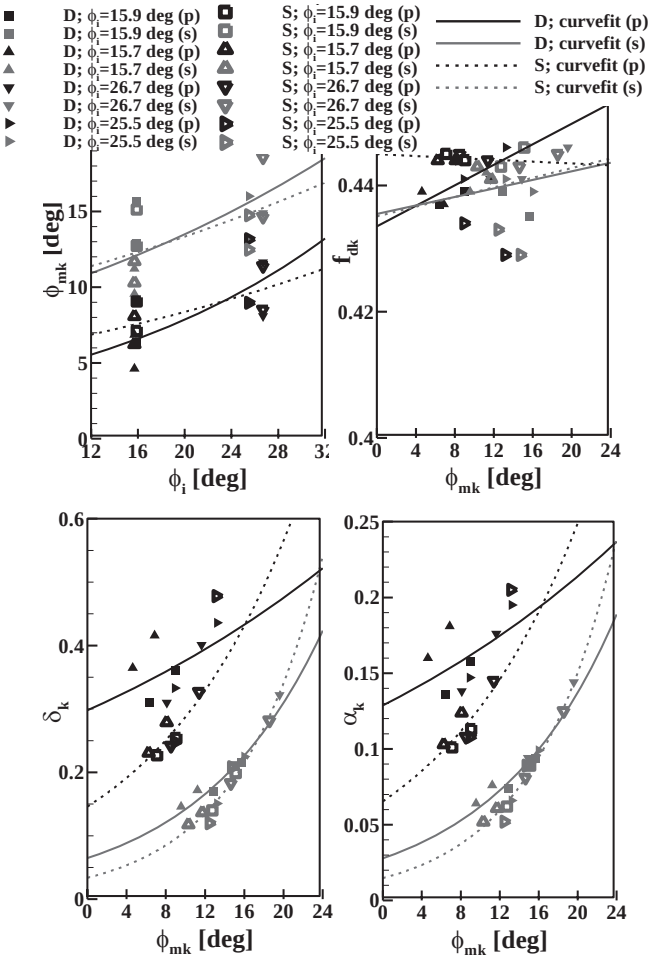

Figure 7 Variation of ϕ_{mk} with respect to ϕ_i and f_{dk},δ_k,α_κ with respect to ϕ_{mk} for damaged roll decay

6. INTACT AND DAMAGED ROLL DECAY

Fig. 5 shows the comparison of the experimental and computational intact condition roll decay ϕ_{mk} vs. ϕ_i and f_{dk}, δ_k and

α_k vs. ϕ_{mk}. f_{dk} changes slightly during roll decay confirming that the restoring moment of the ship is fairly linear. The damped roll frequency is close to roll natural frequency (see Table 1) and about 10% larger than the damped roll frequency in flooding, as explained earlier. Table 3 summarize the values and errors for the validation variables. For f_d, E is <1%D for both intact roll decay cases, showing very good agreement with the experimental data. The E values for linear damping is about 37%D for the intact case with smaller initial roll angle ϕ_i while the error decreases to 16%D for the case with larger ϕ_i. Nonetheless, the results show close agreement with the experimental data as the error for ϕ_m is 4% for the case with smaller ϕ_i, dropping to 2.5% for the case with larger ϕ_i. The simulations display strong roll, sway and yaw coupling for which validation data is not available.

Table 5 CFD and EFD comparison of 1/2, 1st and 2nd harmonic amplitudes for intact SSRC in beam waves with H/λ=1/60

λ/L		0.52			1.17			1.99			2.2			2.42			
		EFD	CFD	E%D	EFD	CFD	E%D	EFD	CFD	E%D	EFD	CFD	E%D	EFD	CFD	E%D	Ave E%D
1st	x/A	0.030	0.034	-13	0.021	0.029	-42	0.017	0.010	39	0.025	0.016	35	0.013	0.015	-14	29
	y/A	0.533	0.525	1	0.673	0.843	-25	1.253	0.864	31	1.349	0.935	31	0.994	0.965	3	18
	z/A	0.936	1.530	-63	1.030	1.081	-5	0.853	0.893	-5	0.772	0.987	-28	0.728	0.978	-34	27
	φ/Ak	0.121	0.201	-66	0.548	0.354	35	4.786	4.720	1	6.297	5.543	12	5.643	5.038	11	25
	θ/Ak	0.022	0.011	49	0.007	0.030	-306	0.049	0.016	67	0.074	0.014	82	0.063	0.014	78	116
	Ψ/Ak	0.005	0.005	-1	0.009	0.019	-101	0.029	0.047	-61	0.046	0.056	-21	0.034	0.050	-48	46
	Avg. E%D			**32**			**86**			**34**			**35**			**31**	**44**
2nd	x/A	0.002	0.000	92	0.001	0.000	77	0.004	0.021	-458	0.011	0.000	95	0.008	0.000	95	163
	y/A	0.003	0.011	-225	0.006	0.012	-121	0.027	0.057	-111	0.119	0.009	92	0.109	0.006	94	129
	z/A	0.001	0.024	-3895	0.007	0.010	-47	0.201	0.059	71	0.150	0.017	89	0.168	0.006	96	840
	φ/Ak	0.003	0.027	-846	0.018	0.017	2	0.045	0.102	-128	0.027	0.057	-110	0.114	0.073	36	224
	θ/Ak	0.000	0.002	-1300	0.002	0.000	94	0.016	0.011	32	0.015	0.002	89	0.007	0.004	41	311
	Ψ/Ak	0.001	0.000	92	0.001	0.000	71	0.010	0.009	11	0.009	0.001	94	0.002	0.001	16	57
	Avg. E%D			**1075**			**69**			**135**			**95**			**63**	**287**
1/2	x/A	0.032	0.010	67	0.013	0.001	91	0.005	0.001	86	0.012	0.000	97	0.005	0.002	53	79
	y/A	5.602	0.565	90	0.004	0.036	-785	0.007	0.007	0	0.012	0.033	-178	0.117	0.007	94	229
	z/A	0.599	0.047	92	0.022	0.020	9	0.029	0.005	83	0.100	0.015	85	0.053	0.008	84	71
	φ/Ak	5.777	7.186	-24	0.007	0.148	-2016	0.044	0.184	-319	0.056	0.092	-64	0.719	0.073	90	503
	θ/Ak	0.069	0.002	97	0.007	0.002	75	0.002	0.001	48	0.010	0.000	96	0.009	0.001	91	81
	Ψ/Ak	0.058	0.044	23	0.001	0.005	-327	0.002	0.009	-475	0.003	0.002	50	0.002	0.004	-96	194
	Avg. E%D			**66**			**550**			**169**			**95**			**85**	**193**
Avg. E%D				**391**			**235**			**113**			**75**			**60**	**175**

Table 6 CFD and EFD comparison of 1/2, 1st and 2nd harmonic amplitudes for damaged SSRC in beam waves with H/λ=1/60

λ/L		0.52			1.17			1.99			2.2			2.42			
		EFD	CFD	E%D	EFD	CFD	E%D	EFD	CFD	E%D	EFD	CFD	E%D	EFD	CFD	E%D	Ave E%D
1st	x/A	0.027	0.040	-49	0.022	0.023	-7	0.015	0.021	-40	0.011	0.017	-55	0.004	0.015	-298	90
	y/A	0.399	0.646	-62	0.573	0.832	-45	0.731	0.852	-17	1.017	0.903	11	1.094	1.053	4	28
	z/A	1.069	1.416	-32	0.966	1.016	-5	0.856	1.032	-21	0.810	1.088	-34	0.859	1.085	-26	24
	φ/Ak	0.140	0.288	-106	0.391	0.572	-46	2.033	1.092	46	4.520	4.388	3	5.539	5.162	7	42
	θ/Ak	0.025	0.033	-31	0.013	0.021	-60	0.013	0.021	-66	0.045	0.013	71	0.065	0.008	87	63
	Ψ/Ak	0.010	0.010	-3	0.009	0.009	-1	0.019	0.022	-15	0.029	0.042	-45	0.038	0.053	-40	21
	Avg. E%D			**47**			**27**			**34**			**37**			**77**	**44**
2nd	x/A	0.005	0.000	93	0.002	0.001	65	0.009	0.002	75	0.003	0.000	91	0.007	0.001	91	83
	y/A	0.004	0.004	10	0.011	0.019	-73	0.049	0.059	-20	0.070	0.018	75	0.119	0.005	96	55
	z/A	0.009	0.013	-36	0.011	0.017	-49	0.126	0.008	94	0.176	0.023	87	0.229	0.054	76	68
	φ/Ak	0.000	0.038	-9263	0.015	0.109	-603	0.066	0.083	-26	0.276	0.161	42	0.036	0.253	-603	2107
	θ/Ak	0.001	0.000	35	0.000	0.003	-809	0.000	0.000	-49	0.013	0.001	89	0.007	0.002	71	211
	Ψ/Ak	0.000	0.000	-35	0.001	0.002	-24	0.004	0.003	23	0.014	0.000	97	0.004	0.004	1	36
	Avg. E%D			**1579**			**271**			**48**			**80**			**156**	**427**
1/2	x/A	0.034	0.001	97	0.021	0.001	96	0.009	0.012	-29	0.002	0.000	78	0.003	0.001	78	76
	y/A	0.505	0.016	97	0.053	0.046	13	0.035	0.065	-84	0.070	0.085	-22	0.006	0.016	-188	81
	z/A	0.116	0.045	61	0.064	0.038	40	0.030	0.018	40	0.066	0.035	48	0.063	0.013	80	54
	φ/Ak	0.558	0.245	56	0.126	0.699	-456	0.143	0.425	-196	0.326	0.491	-51	0.027	0.301	-1019	356
	θ/Ak	0.008	0.001	86	0.004	0.002	40	0.004	0.000	89	0.007	0.001	79	0.002	0.001	23	63
	Ψ/Ak	0.010	0.000	98	0.005	0.009	-72	0.002	0.024	-1391	0.004	0.005	-10	0.002	0.018	-665	447
	Avg. E%D			**82**			**120**			**305**			**48**			**342**	**179**
Avg. E%D				**569**			**139**			**129**			**55**			**192**	**217**

Fig. 6 shows the comparison of the experimental and computational damaged condition roll decay and two compartment wave elevations along with a snap shot of the predicted two compartment flooding. The roll decay and floodwater height time histories show good agreement between the experimental data and CFD.

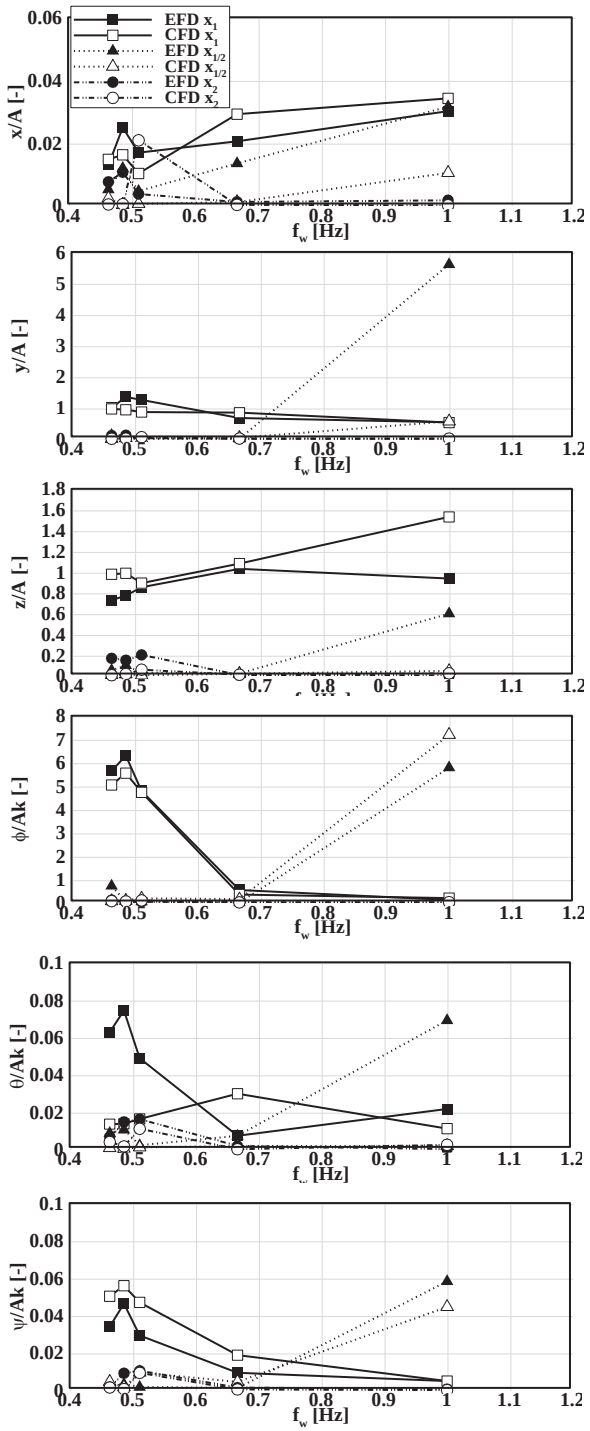

Figure 8 RAO of intact ship motions in beam waves with H/λ=1/60 for different wave frequency

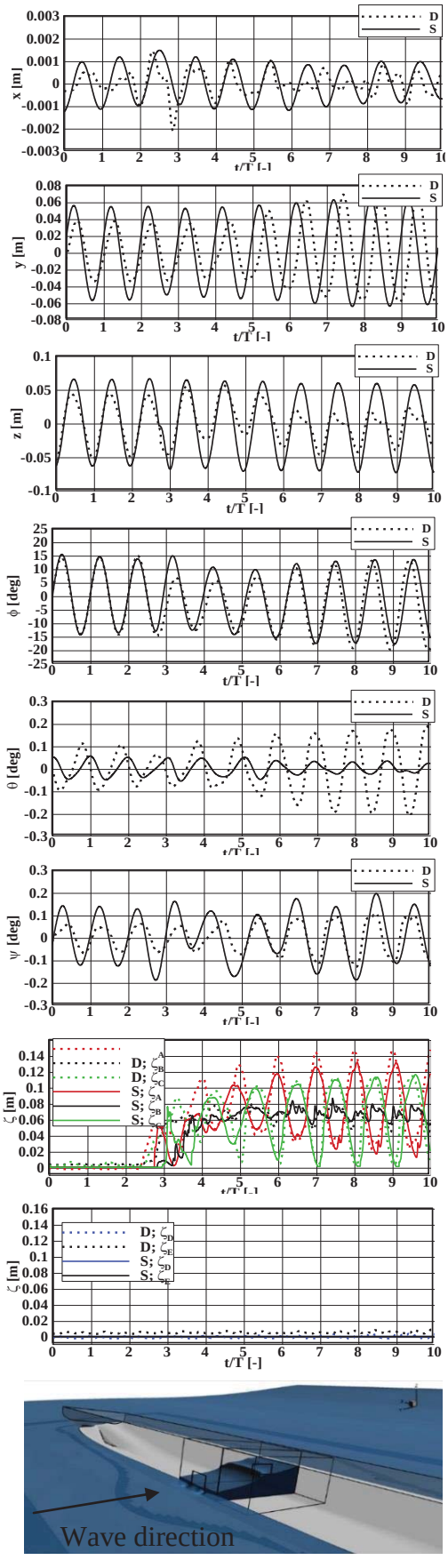

Figure 9 Time history of damaged ship motions in beam waves with λ= 2.42L and H/λ=1/60

Fig. 7 shows the comparison of the experimental and computational damaged condition roll decay ϕ_{mk} vs. ϕ_i and f_{dk}, δ_k and α_k vs. ϕ_{mk}. The experiments and simulations show scatter for the roll decay variables compared to the intact condition. The values are more scattered for portside. Tables 3 and 4 summarize the values and errors for the validation variables. Similarly as for flooding (and intact roll decay) the error for f_d is quite small for all damaged roll decay cases. The error is <2% for the cases with one-room compartment and <6% for the case with two-room compartment, showing much better prediction for current CFD studies compared to the potential flow studies (E~22%D), reported in ITTC (2002). α is mostly under predicted for current CFD simulations, same as for potential flow studies. However, the error values are within 2.4-29%D which is less than those reported for potential flow studies (E~62%D). The current results also show E=10.7-17%D for ϕ_m, E=1.4-10%D for wave frequency and E=1.9-16%D for mean wave elevation. Overall, the simulations are in both qualitative and quantitative agreement with the experiments. The simulations display strong roll, sway and yaw coupling for which validation data is not available. Fig. 6f snap shot of the two compartment flooding shows water entry with sloshing. The sloshing frequency is close to the damped roll frequency as shown in Table 4.

Comparison of the intact and damaged roll decay shows the damped roll frequency is 10%/11% smaller and damping is 15%/45%larger for the damaged ship with one /two -room compartment, which follows the stated trends in ITTC Stability in Waves Committee report (2002). Since the water height in both rooms are quite same, it was expected to have similar effect on the damped roll frequency for both one- and two–room compartment cases. However, the flooding water acts as an anti-rolling tank and damps the roll motion more quickly for the case with larger volume of flooded water. Additionally, the results showed average heel angle of -2.7 deg for one-room compartment and -5.84 deg for two-room compartment cases. The heel angle for one room compartment cases are comparable with the one for the flooding (-2.5 deg).

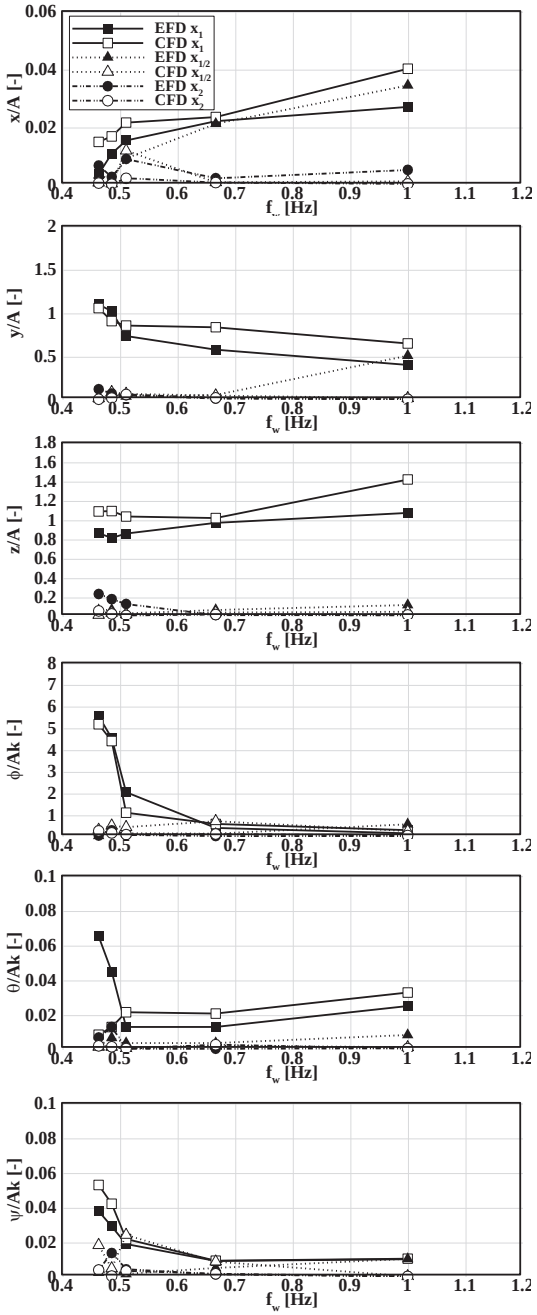

Figure 10 RAO of damaged ship motions in beam waves with H/λ=1/60 for different wave frequency

7. INTACT AND DAMAGED BEAM WAVES

Fig. 8 shows the comparison of the experimental and computational intact beam waves 6DOF 1st order (RAO), ½ and 2nd order responses. Table 5 summarizes the validation variable and E values. All motions show primarily 1st order response, except for parametric roll condition which shows large ½ harmonic response. The peak for roll, sway and yaw responses are at same wave frequency showing strong roll, sway and yaw coupling. The 1st order response for sway, roll and yaw is near the roll resonance condition while their large ½ harmonic response is where the wave frequency is nearly twice of the roll frequency.

The heave 1st order response is quite large z/A=1.0, causing 1st order response for pitch and surge in beam waves due to surge, heave and pitch coupling. The 2nd order responses are small. The E value for 1st order responses is often larger for pitch motion with maximum error for λ/L=1.17, as the EFD value is surprisingly too small for that wavelength condition. Overall, the averaged errors for 1st order responses are quite similar for different wavelength conditions (E~31-35%D) without considering λ/L= 1.17 test case. For ½ and 2nd order responses, the average errors are 63-135%D and 66-169%D, respectively, excluding the large errors often shown for λ/L=0.52 and 1.17. Large E values could be due to the complex mounting system in the experiment. Nonetheless, the simulations are in both qualitative and quantitative agreement with the experiments.

Fig 9 shows the comparison of the experimental and computational damaged ship beam waves roll and flooded compartment wave elevations along with a snap shot of the predicted compartment flooding. Fig. 10 shows the comparison of the experimental and computational damaged beam waves 6DOF 1st order (RAO), ½ and 2nd order responses. Table 6 and 7 summarizes the validation variable E values. All motions show primarily 1st order response. Similarly as for the intact condition, the peaks for roll, sway and yaw responses are located at same wave frequency. Parametric roll (½ harmonic response) is not shown. The 2nd order responses are small. The average E value for 1st harmonic responses is within 27-77%D for different wavelength conditions. Among all motions, the largest errors are often for surge and pitch motions. Even though the average error for 1st harmonic roll amplitude for all the wavelength cases (E=42%D) is quite large, it is still much smaller than the value report for potential flow studies in ITTC report (E~91%D) since the viscous effects are more accurately predicted. Similarly as for the intact condition, ½ and 2nd order variables show larger errors. Large error values could be due to the complex mounting system in the experiment. As shown in Table 7, the mean value of the compartment water height is well predicted with E<6.5%D while ½, 1st and 2nd harmonic amplitudes of the compartment water height show large errors. Nonetheless, the water heights are in both qualitative and quantitative agreement with the experiments, as shown in Fig. 9.

Comparing the intact and damaged ship shows that larger roll damping for the damaged ship reduces the amplitude of 1st order responses. Additionally, the peak for 1st order responses for the damaged ship (roll resonance) occurs at smaller wave frequency (longer wavelength) confirming larger roll period for the damaged ship. Similarly, the peak for ½ order responses (parametric roll) should occur at longer wavelength due to flooding and thus more simulations between λ/L=0.52 and 1.17 are required to resolve the peak for ½ order responses. Unlike the beam wave results for damaged passenger Ro-Ro ship reported in 23rd ITTC report (2002), 2nd order responses were small for SSRC damaged ship.

Table 7 CFD and EFD comparison of water height inside the compartment for beam wave cases

Type	λ/L	EFD/CFD	ζ_A				ζ_B				ζ_C				Ave. $\bar{\zeta}$	Ave. ζ_1	Ave. ζ_2	Ave. $\zeta_{1/2}$	Ave.
			$\bar{\zeta}_A$	ζ_{A1}	ζ_{A2}	$\zeta_{A1/2}$	$\bar{\zeta}_B$	ζ_{B1}	ζ_{B2}	$\zeta_{B1/2}$	$\bar{\zeta}_C$	ζ_{C1}	ζ_{C2}	$\zeta_{C1/2}$					
Damaged beam waves	0.52	EFD	0.079	0.017	0.007	0.005	0.069	0.002	0.006	0.001	0.065	0.016	0.006	0.007					
		CFD	0.076	0.023	0.008	0.002	0.069	0.002	0.009	0.000	0.067	0.022	0.008	0.002					
		E%D	**3.05**	**-34.74**	**-10.63**	**63.96**	**-0.31**	**-64.75**	**-50.07**	**62.16**	**-3.22**	**-39.41**	**-24.89**	**63.71**	**2.20**	**46.30**	**28.53**	**63.28**	**35.08**
	2.20	EFD	0.077	0.050	0.003	0.007	0.067	0.002	0.005	0.000	0.060	0.052	0.007	0.006					
		CFD	0.086	0.047	0.008	0.005	0.069	0.006	0.002	0.001	0.063	0.051	0.007	0.005					
		E%D	**-10.45**	**4.28**	**-189.37**	**26.95**	**-4.06**	**-261.22**	**61.63**	**-53.63**	**-5.08**	**3.41**	**6.34**	**29.23**	**6.53**	**89.63**	**85.78**	**36.60**	**54.64**
	2.42	EFD	0.074	0.055	0.002	0.003	0.066	0.004	0.006	0.000	0.064	0.057	0.008	0.004					
		CFD	0.078	0.060	0.009	0.000	0.066	0.011	0.004	0.001	0.067	0.056	0.011	0.001					
		E%D	**-5.38**	**-8.35**	**-377.56**	**92.59**	**-0.31**	**-189.50**	**38.89**	**-119.14**	**-4.55**	**1.93**	**-36.41**	**82.16**	**3.41**	**66.59**	**150.95**	**97.96**	**79.73**

8. CONCLUSIONS AND FUTURE RESEARCH

URANS capabilities are assessed for zero-speed ship flooding using experimental validation data for flooding and roll decay in calm water and regular beam waves at zero speed.

For flooding and roll decay, the simulations show the ability to predict the trend of increases in roll period and damping due to flooding, as reported in ITTC (2002). The damping magnitudes were often under-predicted similar to potential flow studies reported in ITTC (2002). However, the errors are smaller for current CFD studies (E<43%D) compared to those reported for potential flow (E~62%D) even thought the computational cost is larger. The damped roll frequency and floodwater heights were well predicted with E<5.5%D and E<7%D, respectively. Therefore, CFD could predict the hydrodynamic added moment of inertia due to the flooding unlike the potential flow as reported in ITTC (2002). Two-room compartment simulation showed three times larger damping than one-room compartment cases whereas the roll period was similar for both conditions. The simulations display strong roll, sway and yaw coupling for which validation data is not available. The compartment showed sloshing with a frequency close to the damped roll frequency for all calm water cases.

For the beam wave cases, all motions show primarily 1st order response, except for the parametric roll condition which shows large ½ harmonic response for the intact ship. The 2nd order responses are small for both the damaged and intact ship, unlike ITTC (2002). The average error for 1st order responses is 44%D with large errors for the intact ship pitch motion and damaged ship surge and pitch motions. The results show that the average error for 1st harmonic roll amplitude (E=42%D) is much smaller than that for potential flow studies in ITTC (2002) (E~91%D) since the viscous effects are more accurately predicted. ½ and 2nd order variables show also large errors. Large error values could be due to the complex mounting system in the experiment. The compartment water height mean value was predicted very well (E<6.5%D) while ½, 1st and 2nd order water height amplitude show large errors. The trend of responses against the wave frequency is similar for sway, roll and yaw motions and also for surge, heave and pitch motions due to the strong coupling between them. For the damaged ship, the larger roll period and damping shift the peak of responses to smaller wave frequency and also reduce the amplitude of responses.

In future, the damaged ship behavior in beam waves approaching the ship from the intact side will be studied. Additionally, damaged stability for the self-propelled free running ship in following or head waves will be investigated.

9. ACKNOWLEDGEMENTS

The research was sponsored by the US Office of Naval Research (ONR) grant 000141-41-04-6-5 and ONR Global as part of the Naval International Cooperative Opportunities in Science and Technology Program (NICOP) under the supervisions of Drs. Ki-Han Kim and Woei-Min Lin. The CFD simulations were conducted utilizing DoD HPC.

10. REFERENCES

Gao, Q., Vassalos, D., 2011, Numerical study of the roll decay of intact and damaged ships. In: 12th STAB workshop, Washington, US.

Gao, Z., Gao, Q., Vassalos, D., 2011, Numerical simulation of flooding of a damaged ship, Ocean Engineering, Volume 38, Issues 14–15, Pages 1649–1662.

Gao, Z., Gao, Q., Vassalos, D., 2013, Numerical study of damaged ship flooding in beam seas. Ocean Eng. 61, 77-87.

Huang J., Carrica P., Stern F., 2008, ,Semi-coupled air/water immersed boundary approach for curvilinear dynamic overset grids with application to ship hydrodynamics,, International Journal Numerical Methods Fluids, Vol. 58, pp. 591-624.

Irvine, M., Longo, J., Stern, F., 2013, Forward Speed Calm Water Roll Decay for Surface Combatant 5415: Global and Local Flow Measurements, Journal of Ship Research, Vol. 57, 2013.

ITTC, 2002, The Specialist Committee on Prediction of Extreme Ship Motions and Capsizing, Proceedings of 23rd International Towing Tank Conference, Venice, 2002.

Lee S., You J.M, Lee H.H., Lim T., Park S.T., Seo J., Rhee S.H., and Rhee K.P., 2015, Experimental Study on the Six Degree-of-Freedom Motions of a Damaged Ship Floating in Regular Waves, IEEE Journal of Oceanic Engineering, DOI:10.1109/JOE.2015.2390751.

Lee S., You J.M, Lee H.H., Lim T., Rhee S.H., and Rhee K.P., 2012, Preliminary Tests of a Damaged Ship for CFD Validation, International Journal of Naval Architecture and Ocean Engineering, Vol. 4, No. 2, pp.172-181.

Lim, T., Seo, J., Park, S.T., Rhee, S.H., 2014, Experimental Study on the Safe-Return-to-Port of a Damaged Ship in Head Seas, 30th SNH, Hobart, Australia.

Palazzi, L., De Kat, J. O., (2004). "Model experiments and simulations of a damaged ship with air flow taken into account", Marine Technology, 41 (1), 38-44.

Papanikolaou, A., Zaraphonitis, G., Spanos, D., Boulougouris, E., Eliopoulou, E., (2000). "Investigation into the capsizing of damaged Ro- Ro passenger ships in waves", Proc. of the 7th Intl Conf on Stability of Ships and Ocean Vehicles, STAB2000, Tasmania, pp. 351-362.

Stern, F., Wilson, R. V., Coleman, H. W., and Paterson, E. G., 2001, Comprehensive Approach to Verification and Validation of CFD Simulations—Part 1: Methodology and Procedures, ASME J. Fluids Eng., 123(4), pp. 793–802.

Strasser, C., Jasionowski, A., Vassalos, D., 2009, Calculation of the time-to-flood of a box shaped barge by using CFD. In: 10th STAB conference, St. Petersburg, Russia.

Xing, T. and Stern, F., 2010, Factors of Safety for Richardson Extrapolation, ASME Journal of fluids engineering, Vol. 132, No. 6, DOI: 061403.

This page is intentionally left blank